Recent Progress on Indoor Organic Photovoltaics: From Molecular Design to Production Scale

*Mathieu Mainville and Mario Leclerc**

Department of Chemistry, Université Laval, Quebec City, Qc G1V 0A6, Canada

Mario Leclerc

Mario.leclerc@chm.ulaval.ca

ABSTRACT

Recently, indoor photovoltaics have attracted much interest for their ability to power small electronic devices and sensors, especially with the growth of the Internet of Things (IoT). Due to their absorption covering ambient emission spectra and tunable electronic structures, π-conjugated polymers and small molecules are well-suited for these applications. Among many benefits, including their ink processability, lightweight and flexibility; indoor organic photovoltaics (IOPVs) show power conversion efficiencies (PCE) over 26%. It represents a power output over 30 μW cm^{-2} under office light (500 lux), which is sufficient to operate many electronic devices and sensors with a relatively small photovoltaic area. This focus review highlights the major advances in the material design for IOPVs and includes some industrial insights to reach the production scale criteria.

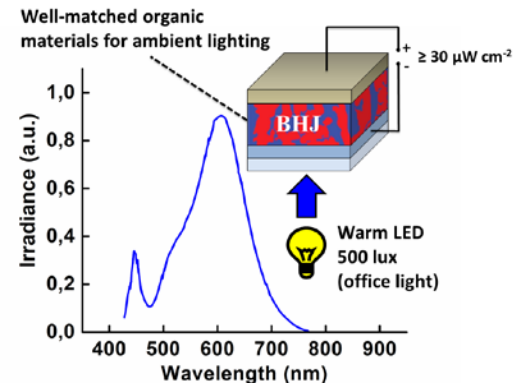

MAIN TEXT

In the past few years, integrated electronics emerged into many fields, ranging from packaging industry to medical activities. Those electronic devices can collect data without human interaction by using sensors. This forms large networks of connected items, commonly called the Internet of Things (IoT). However, these small electronic devices require small amount of energy to operate. Yet, batteries have a restricted lifetime, which limits their range of applications. Photovoltaic (PV) cells are ideal candidates as sustainable power sources for those multiple devices. Although standard silicon PVs show interesting properties for large-scale energy harvesting applications, they compose many problems when it comes to small, lightweight and portable devices for the IoT. They also present a lack of efficiency under ambient (indoor) lighting, where many devices are used.[1] In the last decades, organic photovoltaic (OPV) devices were deeply studied in parallel to their inorganic counterparts. Their lightweight, low cost and flexibility makes them ideal for portable devices.[2] The active materials can be processed as ink and printed through large scale deposition methods, such as roll-to-roll coating. The active layer is usually composed of a blend of *n*-type (electron acceptor) and *p*-type (electron donor) semiconductors, forming a bulk heterojunction (BHJ)[3-5]. Due to the short diffusion length of excitons in organic semiconductors, this nanoscale morphology maximizes their dissociation, thus charge collection to the electrodes.[6] The bandgap (E_g) of both type semiconductors composing the active layer can easily be tuned to

match the emission spectrum of commonly used light-emitting diodes (LED) or fluorescent (FC) lights. Furthermore, it has been shown that OPV cells are more efficient under variable incident light angles, which is not the case for silicon photovoltaic cells.[7, 8] This aspect is important for portable devices, where the incident light angle can fluctuate. Up to date, the most efficient indoor organic photovoltaic (IOPV) cells have power conversion efficiencies (PCEs) over 26% under FC or LED.[9-12] It allows a power output over 30 μW cm^{-2} under 500 lux of indoor illumination, which is enough to power sensors and communication devices with a small photovoltaic area. In comparison, crystalline silicon (c-Si) can achieve PCEs of 20% under LED illumination.[13]

Based on these benefits, conjugated materials are continuously adapted for indoor applications. A hype for indoor photovoltaic technologies for the IoT has been observed over the last 5 years, as the number of reports mentioning both technologies increases following a similar trend (Figure 1). The progress in the material design for IOPVs will be the topic of this focus review.

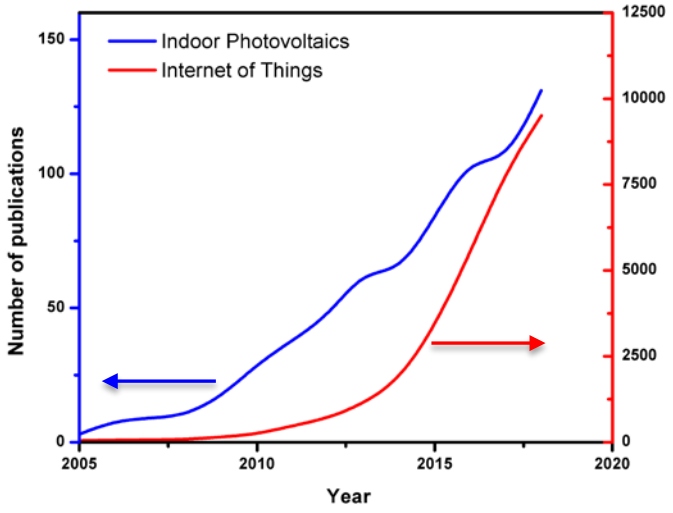

Figure 1: Graph of the number of publications with mention of ‘‘Indoor Photovoltaics’’ and ‘‘Internet of Things’’ over the last decades. Data were taken from Web of Science database on January 6th, 2020.

Material and device specifications for IOPVs

Material design for IOPVs differs slightly from that developed for organic solar cells (OSCs). First, common light sources like FC and LED emit from 400 to 700 nm, equivalent to energies between 1.8 and 3.0 eV (Figure 2). Conjugated semiconductors must then have absorption covering this region. Furthermore, the light intensity from indoor radiance is about 100 to 1000 times lower than the sunlight. Therefore, a lower current density (Jsc) is produced from these devices, due to a lower charge generation. This factor decreases the charge recombination rate and consequently, the fill factor (FF) of the device increases.[14] The thickness of the active layer also has less impact on the FF. The thickness independence is crucial for the large-scale production of organic solar cells, where roll-to-roll printing is considered as the main deposition method.[15-17] This printing technique is less accurate in term of thicknesses than the usual spin coating method used in laboratory scale.[18] Furthermore, the open-circuit voltage (V_{OC}) is affected by the lower incident light intensity.[19-23] It decreases as function of the logarithm of the device photocurrent, expressed as

$$V_{OC} \approx \frac{nkT}{e} ln \frac{I_{ph}}{I_{dark}} \quad (1)$$

where *n* is the ideality factor, *k* the Boltzman constant, T the temperature, *e* the elementary charge, I_{dark} the dark current and I_{ph} the photocurrent. It can be deduced from equation 1 that higher V_{OC} are obtained with materials leading to low dark current, i.e. high bandgap semiconductors.[24-26] Thus, the V_{OC} reduction (ΔV) between indoor and outdoor illumination can be estimated as

$$\Delta V \approx \frac{nkT}{e} ln \frac{I_{ph,sun}}{I_{ph,indoor}}. \quad (2)$$

Further estimations of the light dependence on ΔV have been explained by So and coworkers,[19] by eliminating the impact of infrared light absence in common indoor lighting. More precisely, it is estimated that the energy loss is around 0.2 eV higher under ambient lighting,[9, 27] where

$$E^{loss} = E_g - eV_{OC}. \quad (3)$$

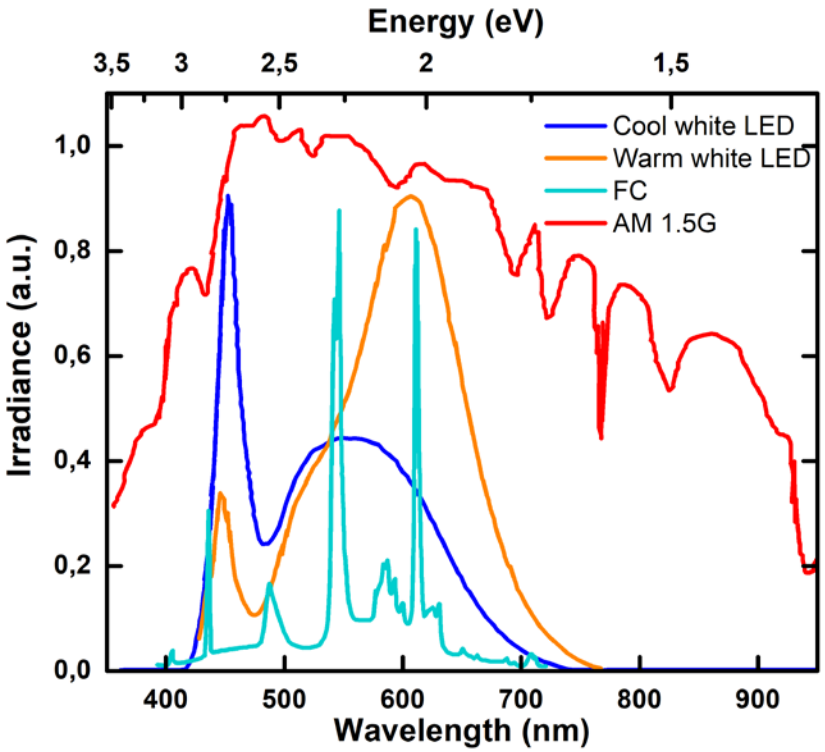

Figure 2: Spectral emission of common ambient light sources and the solar spectrum at AM 1.5G. (Data were plotted from Hou *et al.*[9, 28] and the energy axis was calculated from the Planck-Einstein relation)

Another issue related to ambient lighting of organic photovoltaic cells is the light-soaking of metal-oxide as electron transporting layer (ETL), commonly ZnO or TiO_X. These ETL are utilized in inverted architectures, which are often prioritized due to their higher stability.[29] However, such

devices have to be exposed to UV light in order to reduce the energy barrier between the work function of ITO and the conductive band of the ETL.[30] Because of the lack of UV radiance from ambient light, it results in a major decrease of the FF. Some reports demonstrated a reduction of the light-soaking issue by doping the ZnO ETL with salts[31, 32] or metals,[33] which could be used for IOPVs. It was also shown recently that the addition of polyethyleneimine ethoxylated (PEIE) on top of the ZnO layer could increase the FF and solve this issue for IOPVs.[34]

Donor materials for fullerene-based IOPVs

Recently, Chung *et al*.[10] demonstrated the first IOPV cell with efficiencies superior to 25% with a small molecule called BTR (Figure 3), previously developed by Jones and coworkers.[35] When processed with the wide-bandgap $PC_{71}BM$ as electron acceptor, PCEs up to 26.2% were obtained under 200 lux and 28.1% under 1000 lux of FC illumination (Table 1). The relatively low energy level of the highest occupied molecular orbital (HOMO) of BTR enables a V_{OC} of nearly 1V under one sun, thus a lower fraction of voltage is lost due to the lower light intensity. A V_{OC} of 0.79V was measured under ambient conditions, which represents a ΔV of 0.21V. It was assumed that a post-treatment such as solvent vapor annealing could decrease the V_{OC} of the devices. It is probably due to the increased crystallinity of BTR, leading to a higher HOMO energy level. Nonetheless, such treatment increases the J_{SC}, FF and PCE. BTR is also known to be efficient when processed in non-halogenated solvents and printed by slot-die coating, which is necessary to the large-scale viability of this approach.[36] Slot-die coated photovoltaic cells can be reproduced by roll-to-roll coating more easily.[37]

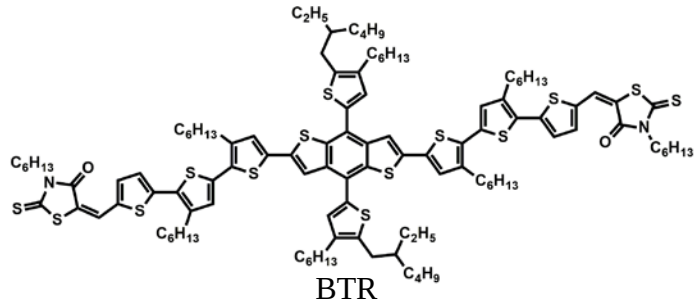

BTR

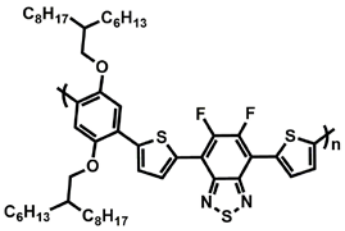

PPDT2FBT

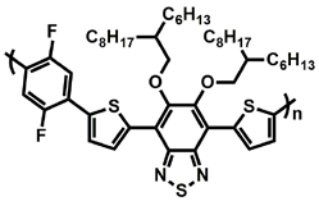

PDTBTBz-2F$_{anti}$

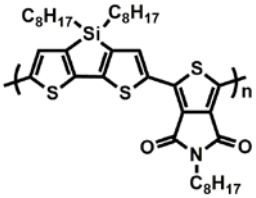

PDTSTPD

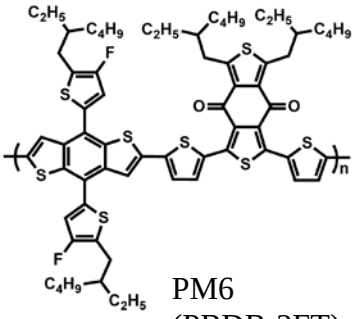

PM6
(PBDB-2FT)

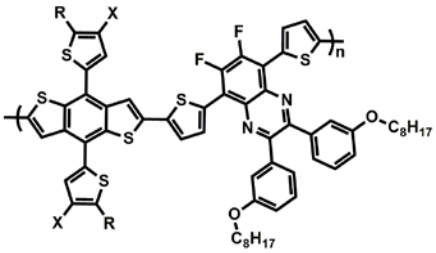

WF3 =X:H, R:2-ethylhexyl
WF3S =X:H, R:2-ethylhexylthio
WF3F =X:F, R:2-ethylhexyl

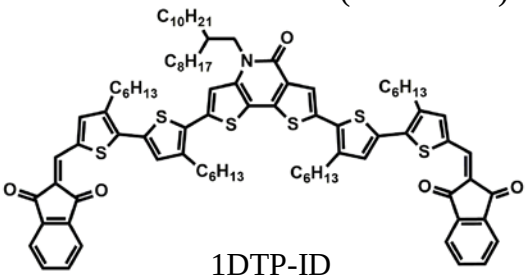

1DTP-ID

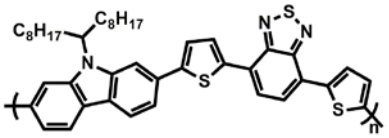

PCDTB

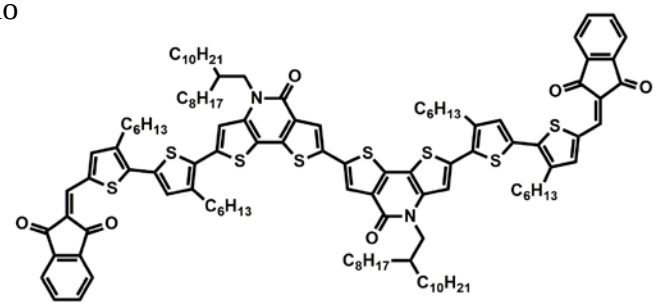

2DTP-ID

Figure 3: Molecular structure of donor materials mentioned for IOPVs.

Table 1: Fullerene-based IOPV results under different illumination

Donor	Fullerene acceptor	Active layer thickness (nm)	Light Source	Light Intensity (lux)	Jsc ($\mu A\ cm^{-2}$)	FF (%)	V_{oc} (V)	P_{out} ($\mu W\ cm^{-2}$	PCE (%)	Ref
BTR	$PC_{71}BM$	220	FC	1000	133	75	0.79	78.2	28.1	[10]
1DTP-ID	PNP	150-190	LED (2900 K)	200	24.6	68	0.67	11.2	19.3	[38]
2DTP-ID	PNP	150-190	LED (2900 K)	200	22.8	63	0.72	10.3	17.8	[38]
PPDT2FBT	$PC_{61}BM$	-	LED (2800 K)	1000	94.6	69.8	0.62	41.3	13.8	[39]
PPDT2FBT	$PC_{71}BM$	280	LED	1000	124.8	56.7	0.579	-	14.6	[40]
PPDT2FBT	$PC_{71}BM$	390	LED	1000	117.1	65.2	0.587	44.8	16.0	[40]
PPDT2FBT	$PC_{71}BM$	760	LED	1000	113.1	59.2	0.574	-	13.7	[40]
PDTBTBz-$2F_{anti}$	$PC_{71}BM$	250	LED	1000	112.4	70.4	0.817	66	23.1	[41]
WF3	$PC_{71}BM$	-	LED	500	58.3	64.2	0.57	-	12.4	[42]
WF3S	$PC_{71}BM$	-	LED	500	60.4	65.7	0.61	-	14.1	[42]
WF3F	$PC_{71}BM$	-	LED	500	63.6	67.4	0.69	-	17.1	[42]
PM6	$PC_{71}BM$	~100	LED (2700 K)	1000	94.1	74.1	0.784	54.7	18.1	[43]
PCDTBT	$PC_{71}BM$	70	FC	300	27.7	69.3	0.72	13.9	16.6	[19]
PCDTBT: PDTSTPD	$PC_{71}BM$	85	FC (2700 K)	300	33.3	63.5	0.73	15.4	20.8	[27]
PTB7-Th	$PC_{71}BM$	-	LED	1000	141.1	44.5	0.57	-	12.79	[11]
PBDB-T	$PC_{71}BM$	-	LED	1000	135.0	48.6	0.61	-	14.24	[11]
PBDB-T: PTB7-Th	$PC_{71}BM$	-	LED	1000	158.0	53.6	0.63	-	19.0	[11]

Additionally, new donor small molecules, namely 1DTP-ID and 2DTP-ID (Figure 3), were specifically designed as indoor light harvesting materials.[38] These materials are based on a dithieno[3,2-*b*:2', 3'-*d*]pyridin-5(4H)-one (DTPO) core, which has weak electron donating properties.[44, 45] The two semiconductors have an optical bandgap of 1.65 eV and 1.70 eV, respectively; which overlaps well with the warm LED (2900 K) emission spectrum. Indeed, the power conversion efficiencies reported for both materials under warm LED illumination approached 20% for 1DTP-ID and 18% for 2DTP-ID. The acceptor material chosen for the BHJ was a pyrrolidine-fused fullerene derivative, PNP,[46] which presents similar electronic properties to $PC_{61}BM$.

Wide bandgap conjugated polymers are also excellent candidates as donor materials for IOPVs. Among the vast choice of semiconductors, PPDT2FBT[47] and PDTBTBz-2F$_{anti}$[48] (Figure 3) show promising properties to reach the industrial scale, both for their simple synthesis and processability. As shown by Welch's group,[39] PPDT2FBT can be processed by slot-die coating in non-halogenated solvents, such as *o*-xylene. Still, it offers a PCE of 13.8% under 1000 lux of warm white LED, when mixed with $PC_{61}BM$ (Table 1). The thickness dependence of the active layer was also studied by Shim *et al*.[40] Interestingly, devices made from PPDT2FBT and $PC_{71}BM$ showed PCEs over 13%, when illuminated by 1000 lux of LED, for active layer with thicknesses varying from 280 to 760 nm. As mentioned earlier, this factor is crucial for up scaling the production of organic photovoltaic cells. In comparison to PPDT2FBT, PDTBTBz-2F$_{anti}$ demonstrates a higher PCE of 23.1% under similar conditions.[41] It can be explained by a high V_{OC} of 0.817V, due to the lower HOMO energy level of the polymer and its larger bandgap.

Moreover, Lee *et al*. designed a series of D – A copolymer based on BDT and quinoxaline subunit.[42] The three polymers, WF3, WF3S and WF3F (Figure 3), are distinct by the variation of

the alkyl side chains and addition of fluorine substituents upon the BDT moiety. The photovoltaic properties of the three polymers blended with $PC_{71}BM$ were studied under indoor and 1 sun conditions. The fluorinated analog shows higher PCEs under both illumination conditions. It was explained that fluorine atoms are effective to reduce the trap-assisted recombination losses. Furthermore, fluorine substitution is well-known for stabilizing the HOMO energy level of conjugated polymers.[49, 50] Thus, both effects increased the V_{OC} of WF3F analog, leading to high PCEs of 17.1% under indoor conditions, compared to 12.4% and 14.1% for WF3 and WF3S, respectively. Those decent efficiencies are also explained by balanced hole and electron mobilities of the polymer:$PC_{71}BM$ blend, which increases the FF and J_{SC}.[51, 52]

Among the most popular *p*-type polymers for OPVs, PBDB-T and its derivatives still show the best PCEs, especially with NFAs under solar simulation.[53-59] The fluorinated homolog, PBDB-T-2F (PM6, Figure 3), showed a PCE up to 17 % in OSC.[54, 60] Its optical bandgap of 1.80 eV is ideal for indoor light absorption and small voltage loss. Hou *et al*. showed interesting performance for 1 cm^2 IOPV devices, where V_{OC} of 0.784V and PCE of 18.1% were obtained under 500 lux of 2700K LED, for a PM6:$PC_{71}BM$ blend. Active areas of 1 cm^2 show more representative photovoltaic characteristics of large-scale modules, since several energetic losses, such as electrical and geometrical losses increase with the size of the cell.[61-64] Additionally, the film inhomogeneity and defects are more recurrent on enlarged areas, which can significantly decrease the efficiencies of the devices.

Another well-suited donor polymer for IOPVs is PCDTBT (Figure 3), known for its high efficiencies in OSC. The deep HOMO energy level and high bandgap lead to a high V_{OC} and good light absorption in the visible spectrum.[65-68] This polymer also has good thermal and photochemical stabilities under outdoor conditions.[69, 70] Due to its low HOMO energy level at -5.5

eV, it is relatively stable against oxidation and high temperatures, which is an important feature for IOPVs. Furthermore, it was an industrial prospect for large-scale photovoltaic modules.[71] It was first studied for indoor applications with $PC_{71}BM$ as electron acceptor material, where PCEs over 16% were measured under 300 lux of FC lighting.[19] Additionally, the PCDTBT:$PC_{71}BM$ system has been reported for a 8 pixels large area module (100 cm^2). Under the same illumination, this IOPV afforded a maximum PCE of 11.2%. This example shows the potential of IOPV on large scale modules. More recently, So and coworkers[27] developped a ternary blend, using PCDTBT and PDTSTPD (Figure 3) as a co-donor material to reach PCEs over 20% under FC illumination. The high efficiencies could be attained due to the low HOMO energy level of the ternary material. V_{OC} of 0.89V under 1 sun and 0.73V under FC or LED lighting can be achieved for this blend. Furthermore, the co-donor PDTSTPD enhances the FF, explained by an increase of hole mobility of the BHJ and more balanced charge mobilities with $PC_{71}BM$.

Additionally, the PTB7-Th:$PC_{71}BM$ (Figure 3) blend is also well-known in the OPV research field, where PCE over 9% can be measured under 1 sun.[72] Under indoor conditions, this blend achieves average PCE of 12.79%.[11] However, by using PBDB-T blended with 10% wt% of PTB7-Th and $PC_{71}BM$, it can attain PCEs up to 18.99%. The second donor material (i.e PTB7-Th) mainly increases the J_{SC}. Compared to the PBDB-T:$PC_{71}BM$ binary system, it improves the PCE by 33%, where PCE up to 14.24% were measured. This is explained by the complementary absorption of PTB7-Th which increases photon absorption. Further optimization of this BHJ with a second acceptor material will be discussed later in this review.

Acceptor materials for IOPVs

Upon the major advances in organic photovoltaics in the past few years, the transition from fullerene to non-fullerene acceptors (NFAs) is clearly the most significant one. Among the improvements to the active layers, NFAs allow better photon absorption in the visible region and easier modulation of the molecular orbital and optical bandgap energies.[73] Consequently, they are ideal candidates for IOPVs, when considering that high V_{OC} of the device is essential. Thus, materials with high bandgaps and relatively high lowest unoccupied molecular orbital (LUMO) energy levels can be designed.

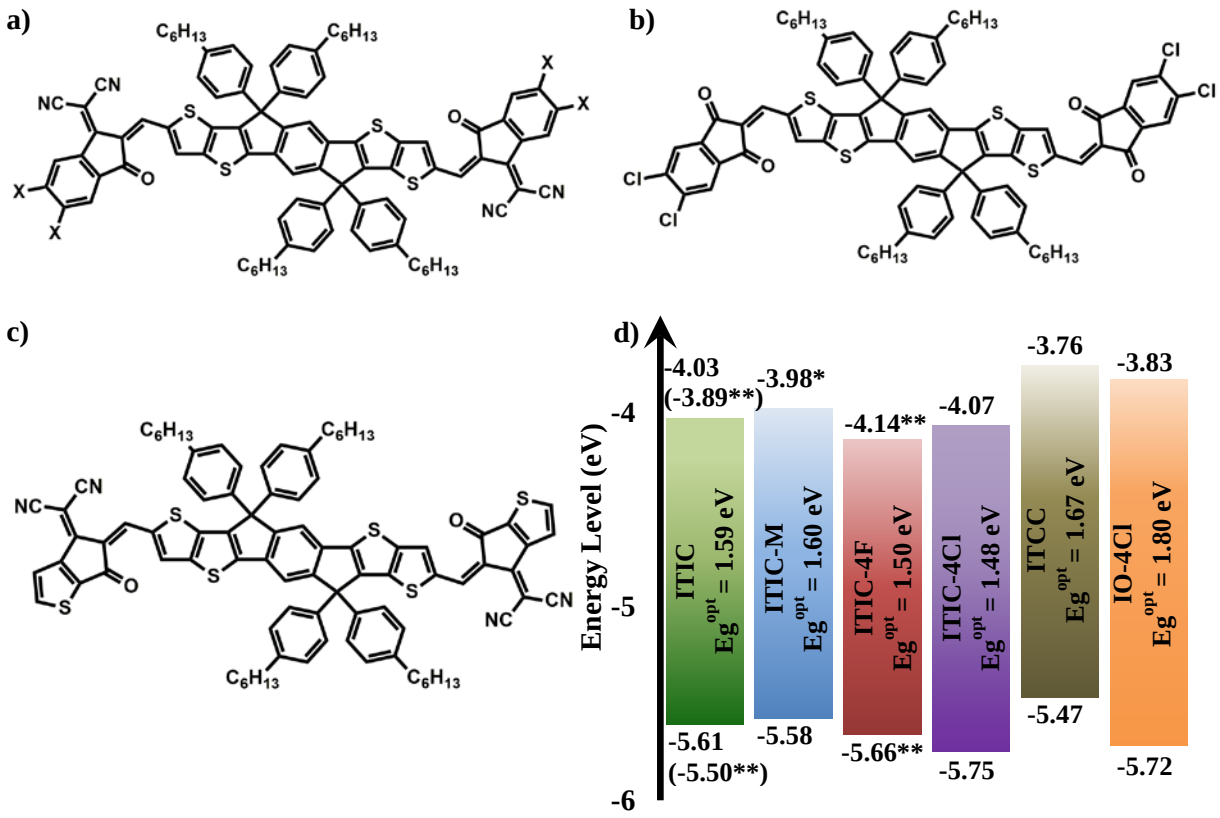

Figure 4: Molecular structures of (a) ITIC (X:H), ITIC-M (X: one methyl and one H on each end group), ITIC-4F (X: F), ITIC-4Cl (X: Cl), (b) IO-4Cl and (c) ITCC. (d) Molecular energy diagram of previous compounds measured by cyclic voltammetry. (*) LUMO level calculated from optical bandgap. (**) Energy level measured from ultraviolet photoelectron spectroscopy (UPS).

Table 2: Non-fullerene based IOPV results under different illumination

Donor	Non-fullerene acceptor	Light Source	Light Intensity (lux)	Jsc ($\mu A\ cm^{-2}$)	FF (%)	Voc (V)	PCE (%)	P_{out} ($\mu W\ cm^{-2}$	Ref
PM6	IO-4Cl	FC (2700 K)	1000	73.8	81.5	1.09	26.4	65.6	[9]
PM6	IO-4Cl	LED (2700 K)	1000	90.6	79.1	1.10	26.1	78.8	[9]
PM6	IT-4F	LED (2700 K)	1000	113	78.0	0.712	20.8	62.8	[43]
PM6	ITCC	LED (2700 K)	1000	95.8	72.2	0.962	22.0	66.5	[43]
PPDT2FBT	ITIC-M	LED (2800 K)	1000	77.4	54.4	0.63	8.9	26.6	[39]
PPDT2FBT	ITIC-F	LED (2800 K)	1000	96.9	37.2	0.45	5.4	16.1	[39]
PPDT2FBT	$TPDI_2N$-EH	LED (2800 K)	1000	66.8	51.0	0.84	9.6	28.7	[39]
PBDB-T	ITIC-Th :$PC_{71}BM$	LED	1000	157	65.1	0.72	26.4	-	[11]
CD1	PBN-10	FC	1000	120	66.2	1.14	26.2	91	[12]

Following that trend, a new NFA named IO-4Cl has been specifically developed by Hou *et al*. for IOPV applications.[9] The material design is based on an A-D-A structure, since this strategy has shown to be promising for NFAs.[74-80] The electron acceptor unit are placed as end groups of the molecular backbone to facilitate the intermolecular electron transfer. IO-4Cl uses the ITIC core (indacenodithieno-[3,2-b]thiophene) as the electron-donating fragment of molecule, which is known for its promising properties for solar cells.[81] The rigid core is composed of two sp^3

hybridized carbon atoms. Due to the steric hindrance of the aromatic side chains, it reduces self-aggregation upon the donor moiety. The fused ring also restrains the rotational disorder, which decreases the reorganization energy. Accordingly, it reduces the energy (and voltage) loss in OPVs.[81-86] In contrast to IT-4Cl,[87] the electron-accepting unit are composed of two carbonyl units, one of which substitutes the more electron-withdrawing malononitrile group (Figure 4). This modification increases the LUMO energy level of the material, therefore the optical bandgap increases from 1.48 to 1.80 eV (Figure 4). When blended with PM6 as donor material, IO-4Cl-based IOPVs attained PCEs over 26% under 1000 lux LED or FC. The stability measurements were also performed under continuous indoor illumination. The photovoltaic cells maintained most of their initial PCE after 1000 hours. Furthermore, large area cells of 4 cm^2 were fabricated for this blend using blade-coating deposition. PCEs up to 23.9 % were measured under the same indoor illumination. The molecular design of IO-4Cl was based on density functional theory (DFT) and time-dependent (TD)-DFT calculations to predict the electrostatic potential and the absorption spectrum.

Indacenodithienothiophene-based NFAs are commonly used for OPV applications.[79, 80, 88] A wide variety of analogs were studied by Hou *et al*.[9, 43] and Welch *et al*.[39] under indoor radiance. As a result, it is possible to compare the impact of the molecular energy levels of the active materials on the photovoltaic properties. First, PM6:ITIC-4F[89] and PM6:ITCC[90] blends were tested and compared under LED illumination. The two NFA structures differ by the presence of the more electron-donating thiophene moiety from the difluorinated benzene on the end groups. This substitution mainly increases the LUMO energy level, thus the bandgap. Interestingly, ITCC and PM6 show HOMO energy levels with nearly the same energy. It has been demonstrated that small HOMO offset leads to small hole driving force between the acceptor and donor materials,

but a reduced E_{loss}.[91-93] Together with its higher bandgap, ITCC-based photovoltaic devices resulted in a high photovoltage of 0.962V and a PCE of 22.0% under 1000 lux of LED, for an active area of 1 cm^2. It is also noted that the ΔV between solar and indoor simulation is only 0.138V, compared to 0.160V for ITIC-4F-based devices. Nonetheless, PM6:ITIC-4F blend showed a higher $J_{SC,}$ but a lower PCE of 20.8% under same environment. The device stabilities were also measured after being continuously illuminated under strong or weak light intensities for 160 hours. The devices kept 90 % of their initial PCE under weak illumination, but only 15% under strong illumination. Very recently, Son and coworkers[94] developed ITIC-4F-based IOPV cells with PM6 and its chlorinated analog PBDB-TSCl (Figure 5). The chlorinated material led to PCE of 21.53% under 500 lux FC illumination. It also exhibited higher thermal stability than PM6. After being heated at 100 °C for 34 hours, PBDB-TSCl only lost 5% of its initial PCE, compared to 25% for the fluorinated counterpart. This is explained by a more stabilized morphology under thermal stress.

A similar comparison has been made between ITIC-4F and ITIC-M[95] with PPDT2FBT as the donor polymer. In contrast to ITIC-4F, ITIC-M possesses electron-donating groups, which increase both the LUMO energy level and the bandgap. Thus, higher V_{OC} were observed under 1000 lux of warm LED for ITIC-M:PPDT2FBT devices, with 0.63V versus 0.45V for ITIC-4F:PPDT2FBT blend. It represents a ΔV of 0.27V and 0.32V, respectively. Moreover, it is interesting to note that all devices were processed via non-halogenated solvents by slot-die coating.

A new NFA based on perylene diimide (PDI) unit was also designed by the same group. PDI is a promising unit to design new NFAs, particularly because of its low cost, strong molar absorption in the visible range, tunable optoelectronic properties and good charge transport.[96-100] $TPDI_2N$-EH (Figure 5) showed a wide optical bandgap of 2.22 eV, leading to photoabsorption between 400 and

600 nm, complementary to PPDT2FBT. Furthermore, the LUMO energy level of -3.6 eV allows a high V_{OC}, where ΔLUMO between donor and acceptor material is only 0.1 eV. Under indoor conditions previously mentioned, $TPDI_2N$-EH:PPDT2FBT blend achieved a V_{OC} of 0.84V, representing a small ΔV of 0.18V. Consequently, the PCE increased by more than 2 fold under ambient conditions, to reach a value of 9.6%. As a comparison, PCEs increased by around 30% for ITIC-M blend and dropped by 30% for ITIC-F blend. Note that higher efficiencies were measured under higher light intensities.

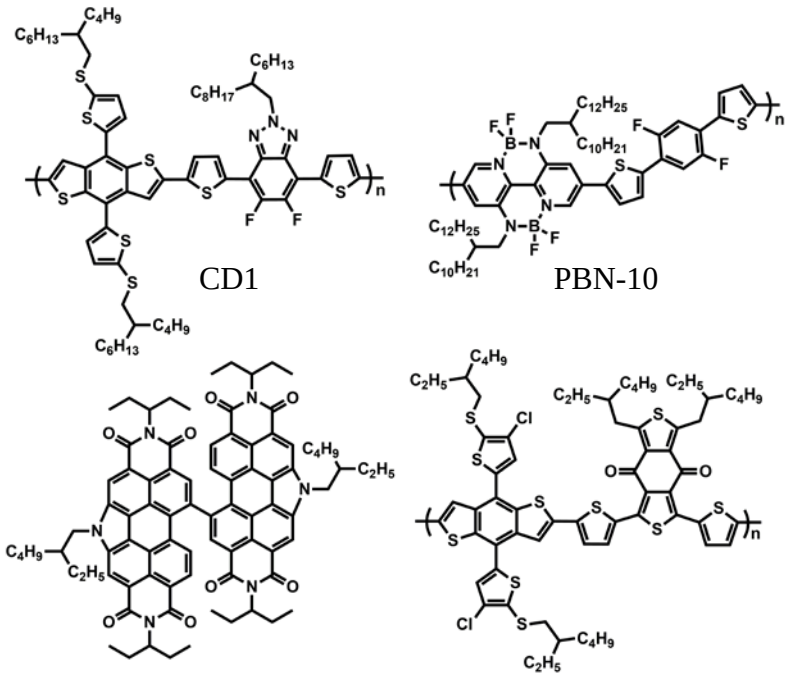

Figure 5: Molecular structure of donor (CD1 and PBDB-TSCl) and acceptor (PBN-10 and $TPDI_2N$-EH) materials mentioned for non-fullerene IOPVs.

Furthermore, all-polymer photovoltaic cells have also shown interesting properties for IOPVs. Liu and coworkers[12] developed an all-polymer blend from CD1[101] (polymer donor) and PBN-10[102]

(polymer acceptor, Figure 5). Both polymers show light absorption below 700 nm, which is ideal for indoor light harvesting applications. A maximum PCE of 26.2% was obtained under 1000 lux of FC lighting, with high V_{OC} of 1.14V.

Finally, a ternary blend based on a 1D:2A BHJ has been developed, using PBDB-T as the *p*-type semiconductor and ITIC-Th[103] and $PC_{71}BM$ as acceptors.[11] It was shown that the NFA enhanced molecular packing and morphology of the active layer, which limits charge recombination. The optimized devices obtained PCEs of 26.4%, with V_{OC} of 0.72V, under 1000 lux LED. Furthermore, the NFA greatly increased the morphological stability of the BHJ under thermal stress. This is explained by the low diffusion of ITIC-Th within the active layer, which therefore maintain the initial morphology. After exposed at 60 °C for 100h, the IOPV devices kept 89.7% of their initial PCE. This aspect is essential as IOPVs move toward production scale.

Design perspectives of indoor organic photovoltaics

Clearly, results discussed in this focus review showed the great potential of π-conjugated materials for indoor photovoltaics. However, only few examples reported novel organic materials specifically designed for IOPVs. Recent developments in the material design of NFAs led to impressive results in OSC.[104] However, most materials used in solar cells must be revised to better fit with the emission spectrum of ambient illumination, mostly by increasing their optical bandgap. Different strategies have already shown to increase the bandgap of NFAs, such as increasing the electronic density of the electron acceptor moieties[9, 95, 105, 106] or by twisting the main-chain in the molecular backbone.[107, 108] Indeed, because the LUMO is mainly located on the end groups, the energy level can be tuned in function of its electronic densities.[75] For example, ITCC shows higher LUMO energy level than ITIC (and slightly higher HOMO energy level), owing to the fused

thiophene (Figure 4). Also, the backbone planarity impacts the electron delocalization upon the molecular structure, which also decreases the bond length alternation (BLA). Both factors reduce the bandgap energy, which is unfavorable for IOPV. Furthermore, most reports mentioned in this focus review showed the importance of the V_{OC} upon the PCE under ambient illumination. Fullerene-based devices often demonstrate a reduced V_{OC} compared to NFA-based IOPVs, explained by higher V_{OC} losses and a better alignment of NFA energy levels with the donor material. It is crucial to target this factor to further increase the efficiencies of IOPV cells. Regarding the device design, one has to look at the energy levels of the semiconductors and their bandgaps to maximize the J_{SC} and V_{OC}. As mentioned earlier, optical bandgaps over 1.7 eV are required to harvest indoor light. Complementary absorptions of donor and acceptor molecules are also necessary to increase the photocurrent. Thus, the addition of a ternary material well-matched for indoor illumination could increase the light absorption and J_{SC} of the IOPV cell.[109] Furthermore, the V_{OC} can be tuned in a multicomponent system by selectively choosing a third component causing an energy cascade alignment.[110, 111] For instance, ternary blend composed of both fullerene and non-fullerene acceptors (e.g. PBDB-T: ITIC-Th/$PC_{71}BM$ blend)[11] could increase both J_{SC}, due the complementary optical gaps of the semiconductors, and V_{OC}, with the better matched electronic levels of NFAs. For the molecular design approach, one promising strategy is based on a decrease of the electron-withdrawing properties of the acceptor fragment in the A-D-A structure,[112] as shown for IO-4Cl. This strategy could be utilized for a wide variety of low bandgap NFAs. It would increase the LUMO energy levels and bandgap; hence higher V_{OC}s would be attainable. For example, the IO-4Cl end group (5,6-dichloro-1H-indene-1,3(2H)-dione) could be used for many NFA cores, like that of the Y6 family.[104] An increase of the bandgap would be expected. Also, a low HOMO energy level for the *p*-type semiconductors is required to

maximized the V_{OC}. One strategy could be the halogenation of these donor materials, which would stabilize both HOMO and LUMO energy levels, while improving the charge transport properties.[49, 113 114]

More importantly, one has to look at industrial requirements for large-scale processing of IOPVs. One of the main aspects sought is the processability of the materials by roll-to-roll coating. Thick-film devices should be prioritized when processed by spin-coating deposition. As shown earlier, IOPV fullerene-based devices may have active layers over 200 nm when exposed to ambient illumination, which is then easier to reproduce by large scale printing methods. This was also reported for IO-4Cl based device,[9] where an active layer of 179 nm could afford PCE of 23.9% under 1000 lux LED. The thickness independence on the photovoltaic performance may be explained by the series/shunt resistance ratio (R_S/R_P), which is related to the charge mobilities and crystallinity of the BHJ.[115, 116] Low or unbalanced charge mobilities lead to space charge accumulation, thus higher recombination for thicker BHJ-based devices.[40, 117-119] However, under low light intensity, this effect decreases. Other scale-up factors were investigated in many studies. Among them, the different deposition processes, the increased module area and the ink deposition in non-toxic solvents are still issues to be solved for large-scale production of OPVs and IOPVs.[120]

Different strategies have been utilized to modulate the solubility of conjugated polymers and small molecules, mainly by modifying the alkyl side chains. For example, the addition of longer side chains or polar side groups on various organic semiconductors has already shown to increase their solubility in non-toxic solvents.[55, 58, 121, 122] High-boiling point solvents and co-solvents are also to be avoided, due to the long drying time at large scale. The processing has to be made under ambient conditions, which includes humidity and oxygen.[123] Thus, the active materials must be

stable under variable environments. Indeed, glovebox-tested materials are not necessarily reproducible at the production scale.

Another very important parameter is the stability of the devices. One of the most important market for IOPVs is the replacement of small batteries powering sensors, so that the maintenance of many wireless devices can be reduced. IOPV devices must be stable for at least 80% of their initial efficiencies for over than 10 years to replace the battery market for the IoT. Furthermore, the PCE of the device should be above 20% under radiance of 500 lux for the targeted applications, resulting in power output around 30 $\mu W\ cm^{-2}$. As previously shown, several IOPV cells already show good stability under indoor illuminations. These promising properties might be explained in part by the absence of UV light and lower radiance in indoor illuminations, which may reduce the "burn-in" effect.[124] It was also shown that C_{60} fullerene can be photo-dimerized, which is unfavorable for the BHJ morphology and efficiencies. Lower light intensity could reduce this undesired reaction. Also, for PBDB-T:$PC_{71}BM$ blend, it was shown that using a ternary non-fullerene component improves the morphological stability of the BHJ. This approach could be used on various polymer:fullerene-based systems. Finally, the transition from spin-coating to larger deposition methods is greatly encouraged as the technology moves forward to large-scale printing. Several devices were made using blade coating or slot-die coating, which are more relevant for industrial processes.

Another issue that needs to be resolved for the development of IOPVs, is the standardization of indoor measurements, *i.e.* the emission spectrum and intensity of the light source. Numerous reports only mentioned results under 1000 lux, which often leads to higher PCEs than with lower radiances, for reasons explained in this focus review. However, radiance of 1000 lux is present mainly in commercial buildings (*e.g.* supermarkets, warehouses). It is not representative for many

devices connected to the IoT. A lower light intensity of 200 to 500 lux would be suggested, as it would better illustrate the photovoltaic properties for the intended applications. As for the light source, a proposal of different spectrum has already been made following photovoltaic simulations.[125] However, by looking at practical applications, LEDs show a longer lifespan and are more energy and cost effective than FC. This light source should be considered as standard for indoor illumination.

In summary, a lot of organic semiconductors have been developed over the last two decades for organic electronics. The insights gained over the years should then allow the design of new materials with the required characteristics for ambient light harvesting applications. Among the next target for IOPV studies, the stability of the devices should be highlighted since this factor is crucial. Ultimately, the main objective is to develop efficient and stable IOPV devices, processed in non-toxic solvents by large-scale deposition methods. As the demand for power sources for the IoT increases, IOPV materials could reach the production-scale quickly if they meet these criteria. We are confident that breakthroughs in the domain will soon lead to devices with PCE approaching 30% under ambient conditions.

BIOGRAPHIES

Mathieu Mainville began in 2017 his graduate studies in chemistry under the supervision of Professor Mario Leclerc and Paul A. Johnson and was awarded both Sentinel North and CERMA Ph.D. Scholarships. His research focuses on the molecular design of new conjugated materials for organic photovoltaics.

Mario Leclerc is the holder of a Canada Research Chair on Electroactive and Photoactive Polymers at Université Laval. He is the author or co-author of more than 275 publications which, according to Google Scholar, already received more than 38 000 citations (h-index of 96).

http://www2.chm.ulaval.ca/profs/mleclerc/public_html/en/index.html

Acknowledgements

The authors acknowledge the Natural Sciences and Engineering Research Council of Canada (NSERC). M. M. thanks Sentinelle Nord (APOGÉE) and the Centre de recherches sur les matériaux avancés (CERMA) for the scholarships. The authors thank François Grenier and Dr. Philippe Berrouard from Brilliant Matters and Dr. Jonas Bergqvist from Epishine for useful discussions.

References

1. Mathews, I.; Kantareddy, S. N.; Buonassisi, T.; Peters, I. M., Technology and Market Perspective for Indoor Photovoltaic Cells. *Joule* **2019,** *3* (6), 1415-1426.

2. Chen, F.-C., Emerging Organic and Organic/Inorganic Hybrid Photovoltaic Devices for Specialty Applications: Low-Level-Lighting Energy Conversion and Biomedical Treatment. *Adv. Opt. Mater*. **2019,** *7* (1), 1800662.

3. Yu, G.; Gao, J.; Hummelen, J. C.; Wudl, F.; Heeger, A. J., Polymer Photovoltaic Cells: Enhanced Efficiencies via a Network of Internal Donor-Acceptor Heterojunctions. *Science* **1995,** *270* (5243), 1789-1791.

4. Halls, J. J. M.; Walsh, C. A.; Greenham, N. C.; Marseglia, E. A.; Friend, R. H.; Moratti, S. C.; Holmes, A. B., Efficient photodiodes from interpenetrating polymer networks. *Nature* **1995,** *376* (6540), 498-500.

5. Lu, L.; Zheng, T.; Wu, Q.; Schneider, A. M.; Zhao, D.; Yu, L., Recent Advances in Bulk Heterojunction Polymer Solar Cells. *Chem. Rev.* **2015,** *115* (23), 12666-12731.

6. Cao, W.; Xue, J., Recent progress in organic photovoltaics: device architecture and optical design. *Energy Environ. Sci.* **2014,** *7* (7), 2123-2144.

7. Mescher, J.; Mertens, A.; Egel, A.; Kettlitz, S. W.; Lemmer, U.; Colsmann, A., Illumination angle and layer thickness influence on the photo current generation in organic solar cells: A combined simulative and experimental study. *AIP Advances* **2015,** *5* (7), 077188.

8. Reynaud, C. A.; Clerc, R.; Lechêne, P. B.; Hébert, M.; Cazier, A.; Arias, A. C., Evaluation of indoor photovoltaic power production under directional and diffuse lighting conditions. *Sol. Energy Mater. Sol. Cells* **2019,** *200*, 110010.

9. Cui, Y.; Wang, Y.; Bergqvist, J.; Yao, H.; Xu, Y.; Gao, B.; Yang, C.; Zhang, S.; Inganäs, O.; Gao, F.; Hou, J., Wide-gap non-fullerene acceptor enabling high-performance organic photovoltaic cells for indoor applications. *Nat. Energy* **2019,** *4* (9), 768-775.

10. Lee, H. K. H.; Wu, J.; Barbé, J.; Jain, S. M.; Wood, S.; Speller, E. M.; Li, Z.; Castro, F. A.; Durrant, J. R.; Tsoi, W. C., Organic photovoltaic cells – promising indoor light harvesters for self-sustainable electronics. *J. Mater. Chem. A* **2018,** *6* (14), 5618-5626.

11. Nam, M.; Kang, J.-h.; Shin, J.; Na, J.; Park, Y.; Cho, J.; Kim, B.; Lee, H. H.; Chang, R.; Ko, D.-H., Ternary Organic Blend Approaches for High Photovoltaic Performance in Versatile Applications. *Adv. Energy Mater.* **2019,** *9* (38), 1901856.

12. Ding, Z.; Zhao, R.; Yu, Y.; Liu, J., All-polymer indoor photovoltaics with high open-circuit voltage. *J. Mater. Chem. A* **2019,** *7* (46), 26533-26539.

13. Cutting, C. L.; Bag, M.; Venkataraman, D., Indoor light recycling: a new home for organic photovoltaics. *J. Mater. Chem. C* **2016,** *4* (43), 10367-10370.

14. Manor, A.; Katz, E. A.; Andriessen, R.; Galagan, Y., Study of organic photovoltaics by localized concentrated sunlight: Towards optimization of charge collection in large-area solar cells. *Appl. Phys. Lett.* **2011,** *99* (17), 173305.

15. Wei, J.; Zhang, C.; Ji, G.; Han, Y.; Ismail, I.; Li, H.; Luo, Q.; Yang, J.; Ma, C.-Q., Roll-to-roll printed stable and thickness-independent ZnO:PEI composite electron transport layer for inverted organic solar cells. *Solar Energy* **2019,** *193*, 102-110.

16. Gasparini, N.; Salvador, M.; Heumueller, T.; Richter, M.; Classen, A.; Shrestha, S.; Matt, G. J.; Holliday, S.; Strohm, S.; Egelhaaf, H.-J.; Wadsworth, A.; Baran, D.; McCulloch, I.; Brabec, C. J., Polymer:Nonfullerene Bulk Heterojunction Solar Cells with Exceptionally Low Recombination Rates. *Adv. Energy Mater.* **2017,** *7* (22), 1701561.

17. Zhang, K.; Chen, Z.; Armin, A.; Dong, S.; Xia, R.; Yip, H.-L.; Shoaee, S.; Huang, F.; Cao, Y., Efficient Large Area Organic Solar Cells Processed by Blade-Coating With Single-Component Green Solvent. *Solar RRL* **2018,** *2* (1), 1700169.

18. Søndergaard, R.; Hösel, M.; Angmo, D.; Larsen-Olsen, T. T.; Krebs, F. C., Roll-to-roll fabrication of polymer solar cells. *Materials Today* **2012,** *15* (1), 36-49.

19. Lee, H. K. H.; Li, Z.; Durrant, J. R.; Tsoi, W. C., Is organic photovoltaics promising for indoor applications? *Appl. Phys. Lett.* **2016,** *108* (25), 253301.

20. Koster, L. J. A.; Mihailetchi, V. D.; Ramaker, R.; Blom, P. W. M., Light intensity dependence of open-circuit voltage of polymer:fullerene solar cells. *Appl. Phys. Lett.* **2005,** *86* (12), 123509.

21. Kirchartz, T.; Deledalle, F.; Tuladhar, P. S.; Durrant, J. R.; Nelson, J., On the Differences between Dark and Light Ideality Factor in Polymer:Fullerene Solar Cells. *J. Phys. Chem. Lett.* **2013,** *4* (14), 2371-2376.

22. Cowan, S. R.; Roy, A.; Heeger, A. J., Recombination in polymer-fullerene bulk heterojunction solar cells. *Physical Review B* **2010,** *82* (24), 245207.

23. Randall, J. F., Designing Indoor Solar Products: Photovoltaic Technologies for AES. **2006**; pp 1-175.

24. Li, N.; Lassiter, B. E.; Lunt, R. R.; Wei, G.; Forrest, S. R., Open circuit voltage enhancement due to reduced dark current in small molecule photovoltaic cells. *Appl. Phys. Lett.* **2009,** *94* (2), 023307.

25. Vandewal, K.; Tvingstedt, K.; Gadisa, A.; Inganäs, O.; Manca, J. V., On the origin of the open-circuit voltage of polymer–fullerene solar cells. *Nat. Mater.* **2009,** *8* (11), 904-909.

26. Elumalai, N. K.; Uddin, A., Open circuit voltage of organic solar cells: an in-depth review. *Energy Environ. Sci.* **2016,** *9* (2), 391-410.

27. Yin, H.; Ho, J. K. W.; Cheung, S. H.; Yan, R. J.; Chiu, K. L.; Hao, X.; So, S. K., Designing a ternary photovoltaic cell for indoor light harvesting with a power conversion efficiency exceeding 20%. *J. Mater. Chem. A* **2018,** *6* (18), 8579-8585.

28. Cui, Y.; Yao, H.; Zhang, J.; Zhang, T.; Wang, Y.; Hong, L.; Xian, K.; Xu, B.; Zhang, S.; Peng, J.; Wei, Z.; Gao, F.; Hou, J., Over 16% efficiency organic photovoltaic cells enabled by a chlorinated acceptor with increased open-circuit voltages. *Nat. Commun.* **2019,** *10* (1), 2515.

29. He, Z.; Zhong, C.; Su, S.; Xu, M.; Wu, H.; Cao, Y., Enhanced power-conversion efficiency in polymer solar cells using an inverted device structure. *Nat. Photonics* **2012,** *6* (9), 591-595.

30. Kim, J.; Kim, G.; Choi, Y.; Lee, J.; Park, S. H.; Lee, K., Light-soaking issue in polymer solar cells: Photoinduced energy level alignment at the sol-gel processed metal oxide and indium tin oxide interface. *J. Appl. Phys.* **2012,** *111* (11), 114511.

31. Yap, C. C.; Yahaya, M.; Salleh, M. M., Effect of organic salt doping on the performance of single layer bulk heterojunction organic solar cell. *Solar Energy* **2011,** *85* (1), 95-99.

32. Ling, Z.; Zhao, Y.; Wang, S.; Pan, S.; Lian, H.; Peng, C.; Yang, X.; Liao, Y.; Lan, W.; Wei, B.; Chen, G., High-performance light-soaking-free polymer solar cells based on a LiF modified ZnO electron extraction layer. *J. Mater. Chem. C* **2019,** *7* (30), 9354-9361.

33. Trost, S.; Zilberberg, K.; Behrendt, A.; Polywka, A.; Görrn, P.; Reckers, P.; Maibach, J.; Mayer, T.; Riedl, T., Overcoming the "Light-Soaking" Issue in Inverted Organic Solar Cells by the Use of Al:ZnO Electron Extraction Layers. *Adv. Energy Mater.* **2013,** *3* (11), 1437-1444.

34. Shin, S.-C.; You, Y.-J.; Goo, J. S.; Shim, J. W., In-depth interfacial engineering for efficient indoor organic photovoltaics. *Appl. Surf. Sci.* **2019,** *495*, 143556.

35. Wong; David J. Jones, K. S.; Zeyun, X.; Shirong, L.; Wojciech, Z.; Wojciech, P.; Eric, H.; Jonathan, M. W.; Rachel, M. W.; Jegadesan, S.; Jianyong, O.; Andrew, B. H.; Wallace, W. H., A molecular nematic liquid crystalline material for high-performance organic photovoltaics. *Nat. Commun.* **2015,** *6* (1), 1-9.

36. Heo, Y.-J.; Jung, Y.-S.; Hwang, K.; Kim, J.-E.; Yeo, J.-S.; Lee, S.; Jeon, Y.-J.; Lee, D.; Kim, D.-Y., Small-Molecule Organic Photovoltaic Modules Fabricated via Halogen-Free Solvent System with Roll-to-Roll Compatible Scalable Printing Method. *ACS Appl. Mater. Interfaces* **2017,** *9* (45), 39519-39525.

37. Po, R.; Bernardi, A.; Calabrese, A.; Carbonera, C.; Corso, G.; Pellegrino, A., From lab to fab: how must the polymer solar cell materials design change? – an industrial perspective. *Energy Environ. Sci.* **2014,** *7* (3), 925-943.

38. Arai, R.; Furukawa, S.; Sato, N.; Yasuda, T., Organic energy-harvesting devices achieving power conversion efficiencies over 20% under ambient indoor lighting. *J. Mater. Chem. A* **2019,** *7* (35), 20187-20192.

39. Dayneko, S. V.; Pahlevani, M.; Welch, G. C., Indoor Photovoltaics: Photoactive Material Selection, Greener Ink Formulations, and Slot-Die Coated Active Layers. *ACS Appl. Mater. Interfaces* **2019,** *11* (49), 46017-46025.

40. Shin, S.-C.; Koh, C. W.; Vincent, P.; Goo, J. S.; Bae, J.-H.; Lee, J.-J.; Shin, C.; Kim, H.; Woo, H. Y.; Shim, J. W., Ultra-thick semi-crystalline photoactive donor polymer for efficient indoor organic photovoltaics. *Nano Energy* **2019,** *58*, 466-475.

41. You, Y. J.; Song, C. E.; Hoang, Q. V.; Kang, Y.; Goo, J. S.; Ko, D. H.; Lee, J. J.; Shin, W. S.; Shim, J. W., Highly Efficient Indoor Organic Photovoltaics with Spectrally Matched Fluorinated Phenylene-Alkoxybenzothiadiazole-Based Wide Bandgap Polymers. *Adv. Funct. Mater.* **2019,** *29* (27), 1901171.

42. Singh, R.; Chochos, C. L.; Gregoriou, V. G.; Nega, A. D.; Kim, M.; Kumar, M.; Shin, S.-C.; Kim, S. H.; Shim, J. W.; Lee, J.-J., Highly Efficient Indoor Organic Solar Cells by Voltage Loss Minimization through Fine-Tuning of Polymer Structures. *ACS Appl. Mater. Interfaces* **2019,** *11* (40), 36905-36916.

43. Cui, Y.; Yao, H.; Zhang, T.; Hong, L.; Gao, B.; Xian, K.; Qin, J.; Hou, J., 1 cm(2) Organic Photovoltaic Cells for Indoor Application with over 20% Efficiency. *Adv. Mater.* **2019,** *31* (42), 1904512.

44. Hao, M.; Luo, G.; Shi, K.; Xie, G.; Wu, K.; Wu, H.; Yu, G.; Cao, Y.; Yang, C., Dithieno[3,2-b:2′,3′-d]pyridin-5(4H)-one-based polymers with a bandgap up to 2.02 eV for high performance field-effect transistors and polymer solar cells with an open-circuit voltage up to 0.98 V and an efficiency up to 6.84%. *J. Mater. Chem. A* **2015,** *3* (41), 20516-20526.

45. Gao, W.; Liu, T.; Hao, M.; Wu, K.; Zhang, C.; Sun, Y.; Yang, C., Dithieno[3,2-b:2′,3′-d]pyridin-5(4H)-one based D–A type copolymers with wide bandgaps of up to 2.05 eV to achieve solar cell efficiencies of up to 7.33%. *Chem. Sci.* **2016,** *7* (9), 6167-6175.

46. Karakawa, M.; Nagai, T.; Adachi, K.; Ie, Y.; Aso, Y., N-phenyl[60]fulleropyrrolidines: alternative acceptor materials to PC61BM for high performance organic photovoltaic cells. *J. Mater. Chem. A* **2014,** *2* (48), 20889-20895.

47. Nguyen, T. L.; Choi, H.; Ko, S. J.; Uddin, M. A.; Walker, B.; Yum, S.; Jeong, J. E.; Yun, M. H.; Shin, T. J.; Hwang, S.; Kim, J. Y.; Woo, H. Y., Semi-crystalline photovoltaic polymers with efficiency exceeding 9% in a ∼300 nm thick conventional single-cell device. *Energy Environ. Sci.* **2014,** *7* (9), 3040-3051.

48. Ko, S.-J.; Hoang, Q. V.; Song, C. E.; Uddin, M. A.; Lim, E.; Park, S. Y.; Lee, B. H.; Song, S.; Moon, S.-J.; Hwang, S.; Morin, P.-O.; Leclerc, M.; Su, G. M.; Chabinyc, M. L.; Woo, H. Y.; Shin, W. S.; Kim, J. Y., High-efficiency photovoltaic cells with wide optical band gap polymers based on fluorinated phenylene-alkoxybenzothiadiazole. *Energy Environ. Sci.* **2017,** *10* (6), 1443-1455.

49. Leclerc, N.; Chavez, P.; Ibraikulov, O. A.; Heiser, T.; Leveque, P., Impact of Backbone Fluorination on pi-Conjugated Polymers in Organic Photovoltaic Devices: A Review. *Polymers* **2016,** *8* (1), 11.

50. Liang, Y.; Feng, D.; Wu, Y.; Tsai, S.-T.; Li, G.; Ray, C.; Yu, L., Highly Efficient Solar Cell Polymers Developed via Fine-Tuning of Structural and Electronic Properties. *J. Am. Chem. Soc.* **2009,** *131* (22), 7792-7799.

51. Wang, J.; Zhang, F.; Zhang, M.; Wang, W.; An, Q.; Li, L.; Sun, Q.; Tang, W.; Zhang, J., Optimization of charge carrier transport balance for performance improvement of PDPP3T-based polymer solar cells prepared using a hot solution. *Phys. Chem. Chem. Phys.* **2015,** *17* (15), 9835-40.

52. Le Corre, V. M.; Chatri, A. R.; Doumon, N. Y.; Koster, L. J. A., Charge Carrier Extraction in Organic Solar Cells Governed by Steady-State Mobilities. *Adv. Energy Mater.* **2017,** *7* (22), 1701138.

53. Yuan, J.; Zhang, Y.; Zhou, L.; Zhang, C.; Lau, T.-K.; Zhang, G.; Lu, X.; Yip, H.-L.; So, S. K.; Beaupré, S.; Mainville, M.; Johnson, P. A.; Leclerc, M.; Chen, H.; Peng, H.; Li, Y.; Zou, Y., Fused Benzothiadiazole: A Building Block for n-Type Organic Acceptor to Achieve High-Performance Organic Solar Cells. *Adv. Mater.* **2019,** *31* (17), 1807577.

54. Lin, Y.; Adilbekova, B.; Firdaus, Y.; Yengel, E.; Faber, H.; Sajjad, M.; Zheng, X.; Yarali, E.; Seitkhan, A.; Bakr, O. M.; El-Labban, A.; Schwingenschlögl, U.; Tung, V.; McCulloch, I.; Laquai, F.; Anthopoulos, T. D., 17% Efficient Organic Solar Cells Based on Liquid Exfoliated WS2 as a Replacement for PEDOT:PSS. *Adv. Mater.* **2019,** *31* (46), 1902965.

55. Cui, Y.; Yao, H.; Hong, L.; Zhang, T.; Xu, Y.; Xian, K.; Gao, B.; Qin, J.; Zhang, J.; Wei, Z.; Hou, J., Achieving Over 15% Efficiency in Organic Photovoltaic Cells via Copolymer Design. *Adv. Mater.* **2019,** *31* (14), 1808356.

56. Sun, H.; Liu, T.; Yu, J.; Lau, T.-K.; Zhang, G.; Zhang, Y.; Su, M.; Tang, Y.; Ma, R.; Liu, B.; Liang, J.; Feng, K.; Lu, X.; Guo, X.; Gao, F.; Yan, H., A monothiophene unit incorporating both fluoro and ester substitution enabling high-performance donor polymers for non-fullerene solar cells with 16.4% efficiency. *Energy Environ. Sci.* **2019,** *12* (11), 3328-3337.

57. Dong, S.; Zhang, K.; Jia, T.; Zhong, W.; Wang, X.; Huang, F.; Cao, Y., Suppressing the excessive aggregation of nonfullerene acceptor in blade-coated active layer by using n-type polymer additive to achieve large-area printed organic solar cells with efficiency over 15%. *EcoMat* **2019,** *1* (1), 12006.

58. Hong, L.; Yao, H.; Wu, Z.; Cui, Y.; Zhang, T.; Xu, Y.; Yu, R.; Liao, Q.; Gao, B.; Xian, K.; Woo, H. Y.; Ge, Z.; Hou, J., Eco-Compatible Solvent-Processed Organic Photovoltaic Cells with Over 16% Efficiency. *Adv. Mater.* **2019,** *31* (39), 1903441.

59. Zhang, S.; Qin, Y.; Zhu, J.; Hou, J., Over 14% Efficiency in Polymer Solar Cells Enabled by a Chlorinated Polymer Donor. *Adv. Mater.* **2018,** *30* (20), 1800868.

60. Cui, Y.; Yao, H.; Hong, L.; Zhang, T.; Tang, Y.; Lin, B.; Xian, K.; Gao, B.; An, C.; Bi, P.; Ma, W.; Hou, J., 17% efficiency organic photovoltaic cell with superior processability. *Natl. Sci. Rev.* **2019**.

61. Hoppe, H.; Seeland, M.; Muhsin, B., Optimal geometric design of monolithic thin-film solar modules: Architecture of polymer solar cells. *Sol. Energy Mater. Sol. Cells* **2012,** *97*, 119-126.

62. Choi, S.; Jr., W. J. P.; Kippelen, B., Area-scaling of organic solar cells. *J. Appl. Phys.* **2009,** *106* (5), 054507.

63. Fan, B.; Zhong, W.; Ying, L.; Zhang, D.; Li, M.; Lin, Y.; Xia, R.; Liu, F.; Yip, H.-L.; Li, N.; Ma, Y.; Brabec, C. J.; Huang, F.; Cao, Y., Surpassing the 10% efficiency milestone for 1-cm2 all-polymer solar cells. *Nat. Commun.* **2019,** *10* (1), 4100.

64. Fan, B.; Zeng, Z.; Zhong, W.; Ying, L.; Zhang, D.; Li, M.; Peng, F.; Li, N.; Huang, F.; Cao, Y., Optimizing Microstructure Morphology and Reducing Electronic Losses in 1 cm2 Polymer Solar Cells to Achieve Efficiency over 15%. *ACS Energy Lett.* **2019,** *4* (10), 2466-2472.

65. Moon, J. S.; Jo, J.; Heeger, A. J., Nanomorphology of PCDTBT:PC70BM Bulk Heterojunction Solar Cells. *Adv. Energy Mater.* **2012,** *2* (3), 304-308.

66. Blouin, N.; Michaud, A.; Leclerc, M., A Low-Bandgap Poly(2,7-Carbazole) Derivative for Use in High-Performance Solar Cells. *Adv. Mater.* **2007,** *19* (17), 2295-2300.

67. Blouin, N.; Michaud, A.; Gendron, D.; Wakim, S.; Blair, E.; Neagu-Plesu, R.; Belletête, M.; Durocher, G.; Tao, Y.; Leclerc, M., Toward a Rational Design of Poly(2,7-Carbazole) Derivatives for Solar Cells. *J. Am. Chem. Soc.* **2008,** *130* (2), 732-742.

68. Park, S. H.; Roy, A.; Beaupré, S.; Cho, S.; Coates, N.; Moon, J. S.; Moses, D.; Leclerc, M.; Lee, K.; Heeger, A. J., Bulk heterojunction solar cells with internal quantum efficiency approaching 100%. *Nat. Photonics* **2009,** *3* (5), 297-302.

69. Cho, S.; Seo, J. H.; Park, S. H.; Beaupré, S.; Leclerc, M.; Heeger, A. J., A Thermally Stable Semiconducting Polymer. *Adv. Mater.* **2010,** *22* (11), 1253-1257.

70. Zhang, Y.; Bovill, E.; Kingsley, J.; Buckley, A. R.; Yi, H.; Iraqi, A.; Wang, T.; Lidzey, D. G., PCDTBT based solar cells: one year of operation under real-world conditions. *Sci. Rep.* **2016,** *6* (1), 21632.

71. Beaupré, S.; Leclerc, M., PCDTBT: en route for low cost plastic solar cells. *J. Mater. Chem. A* **2013,** *1* (37), 11097-11105.

72. Zhang, S.; Ye, L.; Zhao, W.; Liu, D.; Yao, H.; Hou, J., Side Chain Selection for Designing Highly Efficient Photovoltaic Polymers with 2D-Conjugated Structure. *Macromolecules* **2014,** *47* (14), 4653-4659.

73. Yan, C.; Barlow, S.; Wang, Z.; Yan, H.; Jen, A. K. Y.; Marder, S. R.; Zhan, X., Non-fullerene acceptors for organic solar cells. *Nat. Rev. Mater.* **2018,** *3* (3), 18003.

74. Lin, Y.; Wang, J.; Zhang, Z.-G.; Bai, H.; Li, Y.; Zhu, D.; Zhan, X., An Electron Acceptor Challenging Fullerenes for Efficient Polymer Solar Cells. *Adv. Mater.* **2015,** *27* (7), 1170-1174.

75. Wadsworth, A.; Moser, M.; Marks, A.; Little, M. S.; Gasparini, N.; Brabec, C. J.; Baran, D.; McCulloch, I., Critical review of the molecular design progress in non-fullerene electron acceptors towards commercially viable organic solar cells. *Chem. Soc. Rev.* **2019,** *48* (6), 1596-1625.

76. Zhang, G.; Zhao, J.; Chow, P. C. Y.; Jiang, K.; Zhang, J.; Zhu, Z.; Zhang, J.; Huang, F.; Yan, H., Nonfullerene Acceptor Molecules for Bulk Heterojunction Organic Solar Cells. *Chem. Rev.* **2018,** *118* (7), 3447-3507.

77. Cheng, P.; Li, G.; Zhan, X.; Yang, Y., Next-generation organic photovoltaics based on non-fullerene acceptors. *Nat. Photonics* **2018,** *12* (3), 131-142.

78. Zhang, Z.; Yuan, J.; Wei, Q.; Zou, Y., Small-Molecule Electron Acceptors for Efficient Non-fullerene Organic Solar Cells. *Front. Chem.* **2018,** *6*, 414.

79. Lin, Y.; Zhang, Z.-G.; Bai, H.; Wang, J.; Yao, Y.; Li, Y.; Zhu, D.; Zhan, X., High-performance fullerene-free polymer solar cells with 6.31% efficiency. *Energy Environ. Sci.* **2015,** *8* (2), 610-616.

80. Lin, Y.; He, Q.; Zhao, F.; Huo, L.; Mai, J.; Lu, X.; Su, C.-J.; Li, T.; Wang, J.; Zhu, J.; Sun, Y.; Wang, C.; Zhan, X., A Facile Planar Fused-Ring Electron Acceptor for As-Cast Polymer Solar Cells with 8.71% Efficiency. *J. Am. Chem. Soc.* **2016,** *138* (9), 2973-2976.

81. Li, Y.; Gu, M.; Pan, Z.; Zhang, B.; Yang, X.; Gu, J.; Chen, Y., Indacenodithiophene: a promising building block for high performance polymer solar cells. *J. Mater. Chem. A* **2017,** *5* (22), 10798-10814.

82. Liao, X.; Shi, X.; Zhang, M.; Gao, K.; Zuo, L.; Liu, F.; Chen, Y.; Jen, A. K. Y., Fused selenophene-thieno[3,2-b]thiophene–selenophene (ST)-based narrow-bandgap electron acceptor for efficient organic solar cells with small voltage loss. *Chem. Commun.* **2019,** *55* (57), 8258-8261.

83. Liang, N.; Jiang, W.; Hou, J.; Wang, Z., New developments in non-fullerene small molecule acceptors for polymer solar cells. *Mat. Chem. Front.* **2017,** *1* (7), 1291-1303.

84. Yang, Y.; Zhang, Z.-G.; Bin, H.; Chen, S.; Gao, L.; Xue, L.; Yang, C.; Li, Y., Side-Chain Isomerization on an n-type Organic Semiconductor ITIC Acceptor Makes 11.77% High Efficiency Polymer Solar Cells. *J. Am. Chem. Soc.* **2016,** *138* (45), 15011-15018.

85. Yao, H.; Cui, Y.; Yu, R.; Gao, B.; Zhang, H.; Hou, J., Design, Synthesis, and Photovoltaic Characterization of a Small Molecular Acceptor with an Ultra-Narrow Band Gap. *Angew. Chem. Int. Ed.* **2017,** *56* (11), 3045-3049.

86. Singh, R.; Lee, J.; Kim, M.; Keivanidis, P. E.; Cho, K., Control of the molecular geometry and nanoscale morphology in perylene diimide based bulk heterojunctions enables an efficient non-fullerene organic solar cell. *J. Mater. Chem. A* **2017,** *5* (1), 210-220.

87. Zhang, H.; Yao, H.; Hou, J.; Zhu, J.; Zhang, J.; Li, W.; Yu, R.; Gao, B.; Zhang, S.; Hou, J., Over 14% Efficiency in Organic Solar Cells Enabled by Chlorinated Nonfullerene Small-Molecule Acceptors. *Adv. Mater.* **2018,** *30* (28), 1800613.

88. Dai, S.; Zhao, F.; Zhang, Q.; Lau, T.-K.; Li, T.; Liu, K.; Ling, Q.; Wang, C.; Lu, X.; You, W.; Zhan, X., Fused Nonacyclic Electron Acceptors for Efficient Polymer Solar Cells. *J. Am. Chem. Soc.* **2017,** *139* (3), 1336-1343.

89. Zhao, W.; Li, S.; Yao, H.; Zhang, S.; Zhang, Y.; Yang, B.; Hou, J., Molecular Optimization Enables over 13% Efficiency in Organic Solar Cells. *J. Am. Chem. Soc.* **2017,** *139* (21), 7148-7151.

90. Yao, H.; Ye, L.; Hou, J.; Jang, B.; Han, G.; Cui, Y.; Su, G. M.; Wang, C.; Gao, B.; Yu, R.; Zhang, H.; Yi, Y.; Woo, H. Y.; Ade, H.; Hou, J., Achieving Highly Efficient Nonfullerene Organic Solar Cells with Improved Intermolecular Interaction and Open-Circuit Voltage. *Adv. Mater.* **2017,** *29* (21), 1700254.

91. Zhang, J.; Liu, W.; Zhang, M.; Liu, Y.; Zhou, G.; Xu, S.; Zhang, F.; Zhu, H.; Liu, F.; Zhu, X., Revealing the Critical Role of the HOMO Alignment on Maximizing Current Extraction and Suppressing Energy Loss in Organic Solar Cells. *iScience* **2019,** *19*, 883-893.

92. Hou, J.; Inganäs, O.; Friend, R. H.; Gao, F., Organic solar cells based on non-fullerene acceptors. *Nat. Mater.* **2018,** *17* (2), 119-128.

93. Liu, J.; Chen, S.; Qian, D.; Gautam, B.; Yang, G.; Zhao, J.; Bergqvist, J.; Zhang, F.; Ma, W.; Ade, H.; Inganäs, O.; Gundogdu, K.; Gao, F.; Yan, H., Fast charge separation in a non-fullerene organic solar cell with a small driving force. *Nat. Energy* **2016,** *1* (7), 16089.

94. Park, S.; Ahn, H.; Kim, J.-y.; Park, J. B.; Kim, J.; Im, S. H.; Son, H. J., High-Performance and Stable Nonfullerene Acceptor-Based Organic Solar Cells for Indoor to Outdoor Light. *ACS Energy Lett.* **2020,** *5* (1), 170-179.

95. Li, S.; Ye, L.; Zhao, W.; Zhang, S.; Mukherjee, S.; Ade, H.; Hou, J., Energy-Level Modulation of Small-Molecule Electron Acceptors to Achieve over 12% Efficiency in Polymer Solar Cells. *Adv. Mater.* **2016,** *28* (42), 9423-9429.

96. Chen, Y.; Ye, P.; Jia, X.; Gu, W.; Xu, X.; Wu, X.; Wu, J.; Liu, F.; Zhu, Z.-G.; Huang, H., Tuning Voc for high performance organic ternary solar cells with non-fullerene acceptor alloys. *J. Mater. Chem. A* **2017,** *5* (37), 19697-19702.

97. Laventure, A.; Stanzel, S.; Payne, A.-J.; Lessard, B. H.; Welch, G. C., A ring fused N-annulated PDI non-fullerene acceptor for high open circuit voltage solar cells processed from non-halogenated solvents. *Synth. Met.* **2019,** *250*, 55-62.

98. Wang, J.; Peng, J.; Liu, X.; Liang, Z., Efficient and Stable Ternary Organic Solar Cells Based on Two Planar Nonfullerene Acceptors with Tunable Crystallinity and Phase Miscibility. *ACS Appl. Mater. Interfaces* **2017,** *9* (24), 20704-20710.

99. Welsh, T. A.; Laventure, A.; Alahmadi, A. F.; Zhang, G.; Baumgartner, T.; Zou, Y.; Jäkle, F.; Welch, G. C., Borane Incorporation in a Non-Fullerene Acceptor To Tune Steric and Electronic Properties and Improve Organic Solar Cell Performance. *ACS Appl. Energy Mater.* **2019,** *2* (2), 1229-1240.

100. Koenig, J. D. B.; Laventure, A.; Welch, G. C., Harnessing Direct(Hetero)Arylation in Pursuit of a Saddle-Shaped Perylene Diimide Tetramer. *ACS Appl. Energy Mater.* **2019,** *2* (12), 8939-8945.

101. Huang, H.; Bin, H.; Peng, Z.; Qiu, B.; Sun, C.; Liebman-Pelaez, A.; Zhang, Z.-G.; Zhu, C.; Ade, H.; Zhang, Z.; Li, Y., Effect of Side-Chain Engineering of Bithienylbenzodithiophene-alt-fluorobenzotriazole-Based Copolymers on the Thermal Stability and Photovoltaic Performance of Polymer Solar Cells. *Macromolecules* **2018,** *51* (15), 6028-6036.

102. Long, X.; Yao, J.; Cheng, F.; Dou, C.; Xia, Y., Double B←N bridged bipyridine-containing polymer acceptors with enhanced electron mobility for all-polymer solar cells. *Mat. Chem. Front.* **2019,** *3* (1), 70-77.

103. Lin, Y.; Zhao, F.; He, Q.; Huo, L.; Wu, Y.; Parker, T. C.; Ma, W.; Sun, Y.; Wang, C.; Zhu, D.; Heeger, A. J.; Marder, S. R.; Zhan, X., High-Performance Electron Acceptor with Thienyl Side Chains for Organic Photovoltaics. *J. Am. Chem. Soc.* **2016,** *138* (14), 4955-4961.

104. Yuan, J.; Zhang, Y.; Zhou, L.; Zhang, G.; Yip, H.-L.; Lau, T.-K.; Lu, X.; Zhu, C.; Peng, H.; Johnson, P. A.; Leclerc, M.; Cao, Y.; Ulanski, J.; Li, Y.; Zou, Y., Single-Junction Organic Solar Cell with over 15% Efficiency Using Fused-Ring Acceptor with Electron-Deficient Core. *Joule* **2019,** *3* (4), 1140-1151.

105. Li, S.; Ye, L.; Zhao, W.; Zhang, S.; Ade, H.; Hou, J., Significant Influence of the Methoxyl Substitution Position on Optoelectronic Properties and Molecular Packing of Small-Molecule Electron Acceptors for Photovoltaic Cells. *Adv. Energy Mater.* **2017,** *7* (17), 1700183.

106. Yang, K.; Liao, Q.; Koh, C. W.; Chen, J.; Su, M.; Zhou, X.; Tang, Y.; Wang, Y.; Zhang, Y.; Woo, H. Y.; Guo, X., Improved photovoltaic performance of a nonfullerene acceptor based on a benzo[b]thiophene fused end group with extended π-conjugation. *J. Mater. Chem. A* **2019,** *7* (16), 9822-9830.

107. Wang, W.; Zhao, B.; Cong, Z.; Xie, Y.; Wu, H.; Liang, Q.; Liu, S.; Liu, F.; Gao, C.; Wu, H.; Cao, Y., Nonfullerene Polymer Solar Cells Based on a Main-Chain Twisted Low-Bandgap Acceptor with Power Conversion Efficiency of 13.2%. *ACS Energy Lett.* **2018,** *3* (7), 1499-1507.

108. Roncali, J., Molecular Engineering of the Band Gap of π-Conjugated Systems: Facing Technological Applications. *Macromol. Rapid Commun.* **2007,** *28* (17), 1761-1775.

109. Gasparini, N.; Salleo, A.; McCulloch, I.; Baran, D., The role of the third component in ternary organic solar cells. *Nat. Rev. Mater.* **2019,** *4* (4), 229-242.

110. Street, R. A.; Davies, D.; Khlyabich, P. P.; Burkhart, B.; Thompson, B. C., Origin of the Tunable Open-Circuit Voltage in Ternary Blend Bulk Heterojunction Organic Solar Cells. *J. Am. Chem. Soc.* **2013,** *135* (3), 986-989.

111. Mollinger, S. A.; Vandewal, K.; Salleo, A., Microstructural and Electronic Origins of Open-Circuit Voltage Tuning in Organic Solar Cells Based on Ternary Blends. *Adv. Energy Mater.* **2015,** *5* (23), 1501335.

112. Alamoudi, M. A.; Khan, J. I.; Firdaus, Y.; Wang, K.; Andrienko, D.; Beaujuge, P. M.; Laquai, F., Impact of Nonfullerene Acceptor Core Structure on the Photophysics and Efficiency of Polymer Solar Cells. *ACS Energy Lett.* **2018,** *3* (4), 802-811.

113. Olla, T.; Ibraikulov, O. A.; Ferry, S.; Boyron, O.; Méry, S.; Heinrich, B. T.; Heiser, T.; Lévêque, P.; Leclerc, N., Benzothiadiazole Halogenation Impact in Conjugated Polymers, a Comprehensive Study. *Macromolecules* **2019,** *52* (21), 8006-8016.

114. Kini, G. P.; Jeon, S. J.; Moon, D. K., Design Principles and Synergistic Effects of Chlorination on a Conjugated Backbone for Efficient Organic Photovoltaics: A Critical Review. *Adv Mater* **2020**, e1906175.

115. Gasparini, N.; Lucera, L.; Salvador, M.; Prosa, M.; Spyropoulos, G. D.; Kubis, P.; Egelhaaf, H.-J.; Brabec, C. J.; Ameri, T., High-performance ternary organic solar cells with thick active layer exceeding 11% efficiency. *Energy Environ. Sci.* **2017,** *10* (4), 885-892.

116. Liu, Y.; Zhao, J.; Li, Z.; Mu, C.; Ma, W.; Hu, H.; Jiang, K.; Lin, H.; Ade, H.; Yan, H., Aggregation and morphology control enables multiple cases of high-efficiency polymer solar cells. *Nat. Commun.* **2014,** *5* (1), 5293.

117. Kirchartz, T.; Agostinelli, T.; Campoy-Quiles, M.; Gong, W.; Nelson, J., Understanding the Thickness-Dependent Performance of Organic Bulk Heterojunction Solar Cells: The Influence of Mobility, Lifetime, and Space Charge. *J. Phys. Chem. Lett.* **2012,** *3* (23), 3470-3475.

118. Cowan, S. R.; Banerji, N.; Leong, W. L.; Heeger, A. J., Charge Formation, Recombination, and Sweep-Out Dynamics in Organic Solar Cells. *Adv. Funct. Mater.* **2012,** *22* (6), 1116-1128.

119. Clarke, T. M.; Peet, J.; Nattestad, A.; Drolet, N.; Dennler, G.; Lungenschmied, C.; Leclerc, M.; Mozer, A. J., Charge carrier mobility, bimolecular recombination and trapping in polycarbazole copolymer:fullerene (PCDTBT:PCBM) bulk heterojunction solar cells. *Org. Electron.* **2012,** *13* (11), 2639-2646.

120. Prat, D.; Wells, A.; Hayler, J.; Sneddon, H.; McElroy, C. R.; Abou-Shehada, S.; Dunn, P. J., CHEM21 selection guide of classical- and less classical-solvents. *Green Chemistry* **2016,** *18* (1), 288-296.

121. Chen, Z.; Yan, L.; Rech, J. J.; Hu, J.; Zhang, Q.; You, W., Green-Solvent-Processed Conjugated Polymers for Organic Solar Cells: The Impact of Oligoethylene Glycol Side Chains. *acs appl. polym. mater.* **2019,** *1* (4), 804-814.

122. Zhang, S.; Ye, L.; Zhang, H.; Hou, J., Green-solvent-processable organic solar cells. *Materials Today* **2016,** *19* (9), 533-543.

123. Chen, L. X., Organic Solar Cells: Recent Progress and Challenges. *ACS Energy Lett.* **2019,** *4* (10), 2537-2539.

124. Mateker, W. R.; McGehee, M. D., Progress in Understanding Degradation Mechanisms and Improving Stability in Organic Photovoltaics. *Adv. Mater.* **2017,** *29* (10), 1603940.

125. Minnaert, B.; Veelaert, P., A Proposal for Typical Artificial Light Sources for the Characterization of Indoor Photovoltaic Applications. *Energies* **2014,** *7* (3), 1500-1516.

QUOTES

“Up to date, the most efficient indoor organic photovoltaic (IOPV) cells have power conversion efficiencies (PCEs) over 26% under FC or LED. It allows a power output over 30 μW cm^{-2} under 500 lux of indoor illumination, which is enough to power sensors and communication devices with a small photovoltaic area.”

“[…] common light sources like FC and LED emit from 400 to 700 nm, equivalent to energies between 1.8 and 3.0 eV. Conjugated semiconductors must then have absorption covering this region.”

“IOPV devices must be stable for at least 80% of their initial efficiencies for over than 10 years to replace the battery market for the IoT.”